A Letters Journal Exploring the Frontiers of Physics

July 2008

EPL, **83** (2008) 24005
doi: 10.1209/0295-5075/83/24005

www.epljournal.org

Evidence of a boundary layer instability at very high Rayleigh number

F. Gauthier and P.-E. Roche

Institut NEEL, CNRS/UJF - BP 166, F-38042 Grenoble Cedex 9, France, EU

received 30 January 2008; accepted in final form 4 June 2008
published online 10 July 2008

PACS 47.27.te – Turbulent convective heat transfer
PACS 44.25.+f – Heat transfer: Natural convection
PACS 44.20.+b – Boundary layer heat flow

Abstract – In 1997, a Rayleigh-Bénard experiment evidenced a significant increase of the heat transport efficiency for Rayleigh numbers larger than $Ra \sim 10^{12}$ and interpreted this observation as the signature of Kraichnan's "Ultimate Regime" of convection. According to Kraichnan's 1962 prediction, the flow boundary layers above the cold and hot plates —in which most of the fluid temperature drop is localized— become unstable for large enough Ra and this instability boosts the heat transport compared to the other turbulent regimes. Using the same convection cell as in the 1997 experiment, we show that the reported heat transport increase is accompanied with enhanced and increasingly skewed temperature fluctuations of the bottom plate, which was heated at constant power levels. Thus, for $Ra < 10^{12}$, the bottom plate fluctuations can simply be accounted from those in the bulk of the flow. In particular, they share the same spectral density at low frequencies, as if the bottom plate was following the slow temperature fluctuations of the bulk, modulo a constant temperature drop across the bottom boundary layer. Conversely, to account for the plate's temperature fluctuations at higher Ra, we no-longer can ignore the fluctuations of the temperature drop across the boundary layer. These observations, consistent with a boundary layer instability, provide new evidence that the transition reported in 1997 corresponds to the triggering of the Ultimate Regime of convection.

Introduction. – Natural convection forces turbulence in the atmosphere, in the oceans as well as in numerous geophysical, industrial and astrophysical flows. Understanding the convection regimes settling on such large scales is a major scientific challenge, directly impacting our ability to assess heat and mass transfer in the environment, for example. One of the simplest laboratory paradigm to explore the basic mechanisms of turbulent convection is the Rayleigh-Bénard cell. It consists in a horizontal layer of fluid between two isothermal plates imposing a temperature difference Δ destabilizing the fluid. Dimensional analysis shows that the main control parameter in such cells is the Rayleigh number (Ra) which is proportional to Δ and to the cube of the fluid layer height (the complete definition of Ra is given later). Unfortunately, due to this geometrical dependence, the reachable Rayleigh numbers in laboratory experiments are decades smaller than those estimated for environmental flows (typically $Ra \sim 10^{20}$ in the atmosphere for example). Thus, our confidence in extrapolating laboratory findings to such flows depends on the understanding of very high Ra experiments.

Since 1997, a few Rayleigh-Bénard experiments [1–4] reported a significant enhancement of heat transport efficiency across the cell above $Ra \sim 10^{12}$ within Boussinesq conditions. These observations were interpreted as the signature of the "Ultimate Regime" of convection, predicted in 1962 by Kraichnan [5]. Qualitatively, this regime is characterized by the turbulent state of the two boundary layers laying close to each plate but the precise conditions for triggering this boundary layer instability are difficult to predict. The interpretation presented in 1997 [1] was motivated by the observation of an unprecedented heat transfer scaling *vs.* Ra, compatible with the onset of Kraichnan's regime and significantly more efficient than any other observed or predicted scaling. In another paper, the authors of [1] reported another signature of the transition on the local temperature statistics at mid-height within the cell [6]. In 2001, the observation of the asymptotic heat transport

scaling of the Ultimate Regime was reported in a similar cell with a calibrated corrugated surface [2]. For usual velocity turbulent boundary layers, such surfaces are well known to set the viscous sub-layer height constant and thus to reveal the asymptotic transport scaling [7]. This experiment therefore supports the 1997 interpretation of the occurrence of the Ultimate Regime of convection.

A direct experiment test would consist in measuring temperature or velocity time series within the boundary layers. Unfortunately, this is difficult for practical reasons: the thermal boundary layer is very thin (typically smaller than $100\,\mu$m in the experiments discussed above) and its temperature profile is Ra dependent. In this work, we bypass the difficulties of local invasive measurements within the boundary layer using the low-frequency fluctuations of the bottom plate as a probe of the stability of the bottom boundary layer. More precisely, we apply a constant heating power J on the bottom plate and monitor its temperature fluctuations (of order one percent of Δ). We focus on times scales longer than the turn-over time of the mean flow circulation, for which the lack of spatial resolution of the "plate-probe" is not a limitation. We find that above $Ra \sim 10^{12}$, such fluctuations become significantly larger than those in the bulk of the flow, while both have the same intensity for lower Ra. Besides, the probability density function of the bottom-plate temperature becomes increasingly skewed towards negative values above $Ra \sim 10^{12}$, corresponding to more and more frequent intense cooling events. We show that both observations are straightforwardly interpretable by the occurrence of an instability in the boundary layer for $Ra \sim 10^{12}$, which is consistent with the scenario of a transition to the Ultimate Regime of convection.

For reference, we mention that three Rayleigh-Bénard experiments explored Ra larger than 10^{13} and did not find any significant enhancement of the heat transfer [8–10]. In [8], a transition of the local temperature statistics have been reported for $Ra \simeq 10^{11}$ and 10^{13} [11]. In [12], the authors report an enhancement of heat transport at high Ra but, according to the authors themselves, the data are not fulfilling the Boussinesq conditions and therefore are difficult to compare to others. Transient Reynolds averaged Navier-Stokes (TRANS) simulations up to $Ra = 10^{15}$ reported an enhancement of heat transfer above $Ra = 10^{13}$ [13], while Direct Numerical Simulations (DNS) up to $Ra = 2 \cdot 10^{14}$ did not [14]. Yet, the DNS found that "*the friction coefficient* C_f [on the plate] *decreases with the boundary layer Reynolds number* Re *as* $Re^{-1/2}$, *as expected for laminar flows, and departs from it at high* Re, *presumably marking the transition to turbulence*" for $Ra \simeq 10^{12}$.

The reason for such a scatter between results at very high Ra is still not understood and this issue is not addressed in this paper, which focuses on the characterisation of the transited regime. We just note that the laminar-to-turbulent transition of velocity-driven boundary layers is known to be highly sensitive to experimental conditions [15] and the same could remain true for "temperature-driven" boundary layers. Thus, the small differences in Prandtl numbers between experiments, or particularities of the different cells[1] could set the flow in one regime or another, and thus originate an *apparent* contradiction between results

For convenience, we recall here the definitions of the main dimensionless parameters. The Rayleigh number $Ra = (gh^3\alpha\Delta)/(\nu\kappa)$ and the Prandtl number $Pr = \nu/\kappa$ characterize the buoyancy force and the molecular transport properties, where g is the gravity acceleration, Δ is temperature difference across the cell of height h and α, ν, κ are, respectively, the isobaric thermal expansion coefficient, the kinematic viscosity and the thermal diffusivity. The Nusselt number $Nu = Jh/(Sk\Delta)$ characterizes the heat transport efficiency across the cell, where J is the mean heat flux (in practice, the applied Joule heating), k the thermal conductivity of the fluid and S the surface of the plate-fluid interface.

Experimental setup. – The convection apparatus used in the present work has been described in [6]. The fluid is confined in a cylindrical volume of height 20 cm and diameter 10 cm with top and bottom oxygen free high conductivity copper (OFHC) plates of thermal conductivity $1090\,\mathrm{W\,m^{-1}\,K^{-1}}$ at 4.2 K [17]. The seamless stainless-steel side wall is $500\,\mu$m thick and its measured thermal conductance is $327\,\mu\mathrm{WK^{-1}}$ at 4.7 K. Its small parasitic contribution to Nu has been corrected using the correction formula proposed in [18]. The cell is hanging in a cryogenic vacuum: the top plate is cooled by helium bath at 4.2 K through a calibrated thermal resistance (3 W/K at 6 K). Its temperature is regulated by a PID controller and we apply a constant and distributed Joule heating on the bottom plate. The heat leaks from the cell in such set-up (about 200 nW at 4.7 K) are at least 4 decades smaller than this heating and are essentially due to the radiative transfer as shown in [19]. The temperature difference Δ between the plates is measured with 0.1 mK accuracy thanks to a thermocouple; for comparison the smallest Δ used in this work is 18 mK. The cell is filled with ^{4}He which properties are calculated based on Arp and Mc Carty works [20] and later improvements [21]. The cell has been operated for 3 mean density and temperature conditions: $19.15\,\mathrm{kg/m^3}$ at 6.0 K ($Pr \simeq 1.0$), $19.15\,\mathrm{kg/m^3}$ at 4.7 K ($Pr \simeq 1.3$) and $70.31\,\mathrm{kg/m^3}$ at 6.0 K ($Pr \simeq 2.8$). These values are a compromise to obtain the best accuracy of helium properties, a 3 decades range of Ra around $Ra = 10^{12}$ and a limited range of Pr.

We now show that the temperature of the bottom plate T_{plate} is a well-defined and measurable global quantity in such a setup, accounting for the homogeneous

[1] For example, one could speculate that the axi-symmetry breaking of the cell described in [10], which "*prevent azimuthal wandering of the wind*"[16], might favor a large-scale circulation preventing the occurence of the transition.

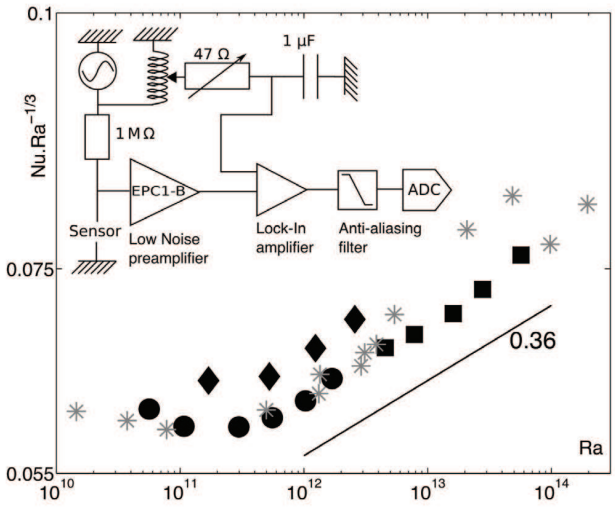

Fig. 1: Compensated *Nu vs. Ra*. Solid symbols: present work, $Pr = 1.0$ (•), $Pr = 1.3$ (♦), $Pr = 2.8$ (■). ∗: data from [6]. Insert: measuring circuit of each thermistance sensor.

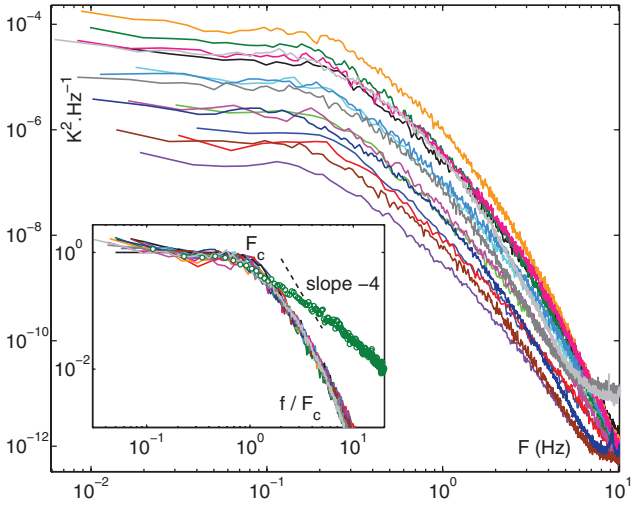

Fig. 2: Power spectra of the bottom-plate temperature T_{plate}. Insert: same spectra normalized by the adjusted plateau value P (y-axis) and by F_c (x-axis). ∘ show a power spectrum of T_{bulk} for $Ra = 1.35 \times 10^{12}$ recorded in a previous run.

temperature fluctuations of the whole plate. Two germanium thermistances are inserted into thermometers holders screwed on this copper plate[2]. The thermal response time of each thermistance is measured with the 3ω technique (for example see [22]). We find cut-off frequencies at -3 dB between 16 Hz and 32 Hz which is consistent with the thermistances' specifications. Thus thermometry has enough dynamics to reflect the plate's temperature fluctuations up to a few Hz, which is above frequencies of interest. The main intrinsic response time of the plate is $\tau_p = d_p^2/\kappa_p$ where $d_p = 10$ cm is the plate's diameter and κ_p is the thermal diffusivity of copper. At 4.7 K, τ_p^{-1} is about 120 Hz which is also larger than the frequencies of interest. Although the plate's diffusive response time is small, the non-homogeneous non-stationary heat fluxes at the fluid-plate interface can still generate temperature gradients in the plate (for example, see [23]). We checked that this effect was negligible for the frequency range of interest: the coherence function between one thermometer located on the cell axis and the other one located on the plate edge is larger than 97% (or 99% if we discard the 3 lowest Δ). T_{plate} is therefore a measurable and well-defined quantity in this setup, at least up to a few Hz.

Each thermistance is polarized with an AC current of a few μA (to prevent significant overheating) and the resulting voltage is demodulated with a lock-in amplifier of 20 ms time constant, connected in a bridge configuration (insert of fig. 1). The output signal is anti-alias filtered and recorded continuously during 5 or 10 h, corresponding typically to a few thousands of turn-over times.

[2]Two different types of thermistances are used on each plate: LakeShore GR-200B-2500 and Cryocal CR1500-PB. Special attention is dedicated to the thermalization using standard cryogenics techniques (Apiezon contact grease, golden copper surfaces, etc. . . .).

Results. – As a preliminary test, we checked that the heat transport law $Nu(Ra)$ across the cell is consistent with the previous measurements with the same apparatus [6], in particular regarding the occurrence of a heat transfert enhancement slightly below $Ra = 10^{12}$. Figure 1 illustrates this agreement by representing the compensated heat transfer $NuRa^{-1/3}$ *vs. Ra* for both experiments (data from [6] are restricted to those for which temperature time series in the bulk are available).

Figure 2 shows the power spectrum density of the bottom-plate temperature T_{plate} for various Ra. At low frequencies, spectra saturate on what we shall refer as "plateaus". These plateaus will be characterized by their spectral densities P. The cut-offs at high frequency are steeper than -3 dB/dec and they can be characterized by the frequencies $F_{20\,\mathrm{dB}}$ at -20 dB below the plateaus, or more conveniently by $F_c = 0.2 \times F_{20\,\mathrm{dB}}$ which roughly corresponds to the cross-over between the plateau and the cut-off regions. In pratice, P has been determined as the value ensuring the best merging of all spectra, when the spectral density is divided by P and the frequency by F_c (solid lines fig. 2 insert). Dimensionless cut-off frequencies $F_c^\star$ and plateaus $P^\star$ are defined by

$$F_c^\star = F_c \cdot h^2/\nu \quad \text{and} \quad P^\star = P \cdot \nu/(h^2\Delta^2), \qquad (1)$$

$F_c^\star$ can be seen as the Reynolds number associated with the distance h and the velocity hF_c. Figure 3 presents this quantity compensated by $Ra^{0.5}$ to illustrate that the scaling of $F_c^\star$ is close to a power law $Ra^{1/2}$ for a given Pr. Similar scalings have already been reported for other Reynolds numbers [6,24] measured in the same window of Ra. In particular, the Reynolds number Re associated with a mean velocity V of the large-scale circulation at

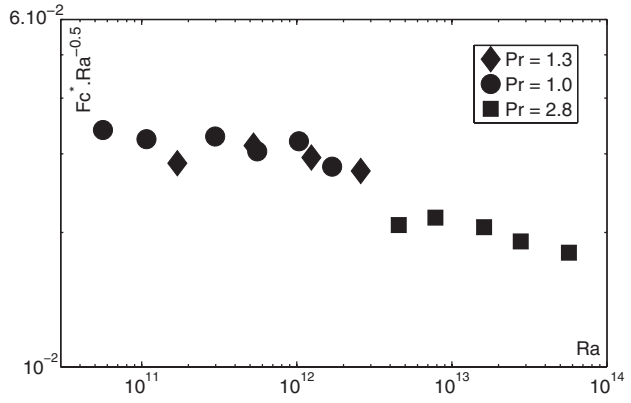

Fig. 3: Compensated cut-off frequency $F_c^\star$ *vs.* Ra.

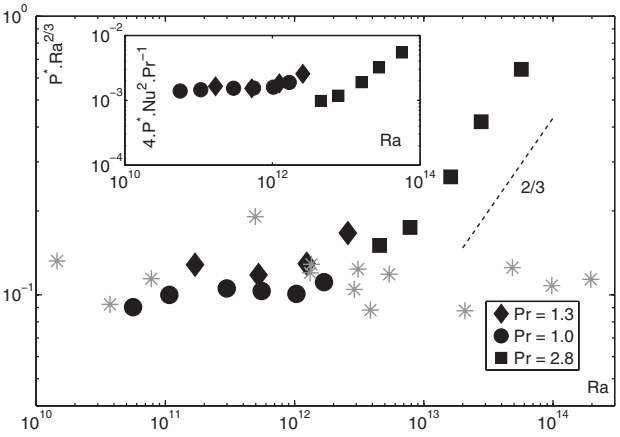

Fig. 4: Compensated plateau level P^* *vs.* Rayleigh number. Solid symbols: temperature fluctations of the bottom plate (same symbols as on fig. 1). *: temperature fluctuations in the bulk of the flow [6]. Insert: alternative normalisation of P (see text).

mid-height (at 2.5 cm from the axis) has been measured and fitted in the present cell as [6]

$$Re = hV/\nu \simeq 0.206 \times Ra^{0.49} Pr^{-0.70}. \qquad (2)$$

The number of turn-overs of the mean flow circulation during a time period $1/F_c$ can be estimated assuming that the circulation path is 2 h long and using the previous mean-velocity V fit. We find $V/2hF_c = Re/2F_c^\star \simeq 2$, indicating that the cross-over between the plateaus and the cut-off region of the T_{plate} spectra is of the order of one turn-over frequency.

The compensated plot of the spectral densities $P^\star$ on fig. 4 is the first important result of this paper. For $Ra < 10^{12}$, the spectral densities dependence $P^\star(Ra)$ is roughly compatible with a $Ra^{-2/3}$ scaling, while it has no obvious Ra dependence for $Ra > 2 \times 10^{12}$, as illustrated by the 2/3 slope (dashed line). For comparison, we also plotted the corresponding spectral density calculated from temperature time series recorded at mid-height within the cell in the previous experiment [6]. Similar spectral

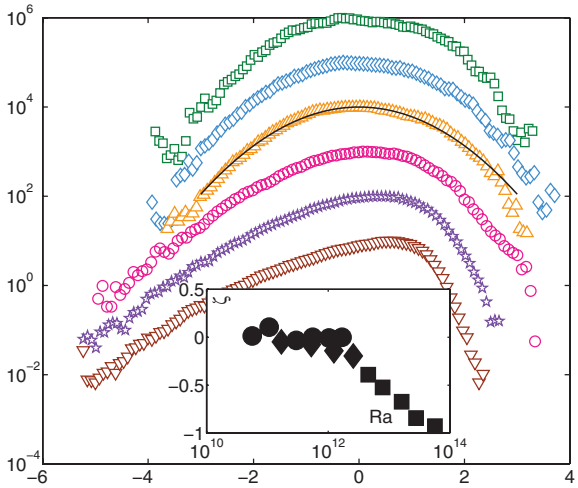

Fig. 5: Probability density functions of $T_{plate} - \overline{T_{plate}}$ normalised by its standard deviation. A vertical offset of one decade is introduced between each datasets. From top to bottom: $Ra = 5.6 \times 10^{10}$ (□), $Ra = 5.5 \times 10^{11}$ (◇), $Ra = 1.7 \times 10^{12}$ (△), $Ra = 4.5 \times 10^{12}$(○), $Ra = 1.6 \times 10^{13}$ (⋆), $Ra = 5.7 \times 10^{13}$ (▽). The insert shows the skewness *vs.* Ra (same symbols as in fig. 1).

plateaus can also be evidenced in these times series below the frequency corresponding to a turn-over time typically. The product $P^\star F_c^\star$ provides an estimate of the standard deviation of the dimensionless temperature fluctuations, which is known to roughly scale like $Ra^{-0.14}$ in the bulk of the flow (for example, see [25]). Since $F_c^\star$ roughly scales like $Re \sim Ra^{0.5}$, we expect $P^\star$ to roughly scale like $Ra^{-0.14-0.5} = Ra^{-0.64}$ in the bulk of the flow, in reasonable agreement with the data. Within experimental uncertainty, the spectral densities plateaus in the bulk overlap with the plate's ones below $Ra = 10^{12}$, but they significantly differ above $Ra = 10^{13}$. The insert shows $4P^\star Nu^2 Pr^{-1}$ *vs.* Ra. This quantity can be seen as P made dimensionless with Δ and the molecular thermal diffusion time across a boundary layer of height $h/(2Nu)$. Within uncertainty, such a compensation of $P^\star$ also cancels the Ra —and maybe Pr— dependences in the low-Ra region. It suggests that the rough $Ra^{2/3}$ scaling of $P^\star$, proposed above for the lower Ra, could be an approximation for a $(Nu(Ra))^2$ scaling.

Figure 5 shows a representative sample of the probability density functions (pdf) of $T_{plate} - \overline{T_{plate}}$ normalized by its standard deviation, where overline stands for time averaging[3]. The Rayleigh numbers range from 5.6×10^{10} (top) up to 5.7×10^{13} (bottom) where vertical offsets are introduced for clarity. The first three pdf are close to Gaussian (the solid line corresponds to a Gaussian distribution), while the others become increasingly skewed as Ra increases: intense coolings of the plate occur more

[3]The Ra-dependence of the dimensionless standard deviation is also steeper above $Ra \sim 10^{12}$ than below, as can be estimated from the product $P^\star F_c^\star$.

and more frequently than the corresponding overheating events. The insert presents the skewness

$$\zeta = \frac{\overline{(T_{plate} - \overline{T_{plate}})^3}}{\overline{(T_{plate} - \overline{T_{plate}})^2}^{3/2}} \quad (3)$$

vs. Ra. It illustrates that the absolute value of the skewness is no longer significantly smaller than unity above $Ra \sim 10^{12}$.

Interpretation. – We assume that, on time scales longer than a few turn-over times, the temperature fluctuations locally recorded in the bulk of the flow reflect temperature variations spanning over the whole bulk of the flow. Accordingly, we interpret the spectral density plateaus of T_{bulk} below F_c as a global characteristics of the bulk temperature, rather than the local one. Since we operate the bottom plate at constant heating power, its temperature T_{plate} is referenced by the fluid's bulk temperature and the temperature drop across the bottom boundary layer. At frequencies smaller than F_c, we can define a time-dependent temperature drop δT_{bl} across the bottom boundary layer, whose mean value is $\Delta/2$ and which fulfills (by definition)

$$T_{plate} = T_{bulk} + \delta T_{bl}. \quad (4)$$

Below $Ra \simeq 10^{12}$, we conjecture that the bottom-plate temperature fluctuations follow the ones of the bulk with negligible noise introduced by the temperature drop δT_{bl} across the bottom boundary layer, that is

$$T_{plate} \simeq T_{bulk} + \Delta/2. \quad (5)$$

This is supported by the overlapping spectral densities plateaus of T_{bulk} and T_{plate} reported on fig. 4. The open circles of the insert of fig. 2 present a typical spectrum of the temperature T_{bulk} for $Ra = 1.35 \times 10^{12}$ and $Pr = 1.3$ recorded during the previous experiment with the same cell. The Y-axis rescaling has been done with the same procedure as previously. The frequency axis is rescaled by $F_c = 0.068\,\mathrm{Hz}$, which was obtained from an interpolation between the solid symbols of fig. 3. The cut-off of the T_{bulk} spectra for $F > F_c$ is less steep than for T_{plate} spectra. This is consistent with a spatial filtering by the plate of the fluid's temperature inhomogeneities extending over less than typically one cell diameter. Estimations of the thermal characteristics of the fluid-plate system also corroborate our conjecture. Indeed, the expected time response of the plate to a slow variation of T_{bulk} can be estimated as RC, where $C \simeq 1\,\mathrm{J/K}$ is the (measured) plate's heat capacity and R is the bottom-boundary-layer dynamical thermal resistance R:

$$R = \frac{\partial \Delta/2}{\partial J} \simeq \frac{1}{1.3}\frac{\Delta/2}{J}. \quad (6)$$

We find that RC is always more than one decade smaller than $1/F_c$. Since the heat capacity of the bottom plate is significantly smaller than the heat capacity of the fluid, the plate represents a negligible thermal load for the slow temperature variations of the bulk fluid. Thus the plate can indeed follow quasistatically the temperature variation of the bulk, modulo the offset introduced by the temperature drop across the boundary layer.

Above $Ra \simeq 2 \times 10^{12}$, the spectral density plateaus $P^\star$ of T_{plate} get increasingly larger than their counterpart in the bulk (fig. 4). We interpret this strong enhancement of fluctuations in the plate as the contribution of the temperature drop δT_{bl} across the boundary layer. At high Ra, the frequent intense cooling events evidenced with the probability distributions of fig. 5 are interpreted considering that the thermal contact between the plate and the bulk is greatly enhanced during short periods of time, corresponding to brief thinning of the boundary layer. The origin of these extra fluctuations is discussed in the next section.

We now discuss and discard the possibility that the phenomenon evidenced above $Ra \sim 10^{12}$ was already present at lower Ra but that the corresponding temperature fluctuations of δT_{bl} were simply masked by the fluctuations of the bulk T_{bulk}. Within this hypothesis of this "masking-effect", fig. 4 could be interpreted without resorting to a flow transition occurring near $Ra \sim 10^{12}$. A first argument is that both enhancements of Nu and T_{plate} fluctuations nearly occur for the same Ra. If we accept that this coincidence is not fortuitous, both events should be accounted by a single mechanism which cannot be a simple masking-effect hypothesis. As a second argument, we note that the strong departure from gaussianity for $Ra > 10^{12}$ is not consistent with the continuous increase of the number of degrees of freedom of the boundary layer expected for the hard-turbulence regime [26], which preceeds the Ultimate one. Indeed, such an increase should favor the convergence to a Gaussian of the pdf of global quantities such as δT_{bl}, which is not the case. Besides, by introducing a shot noise model to account for the temperature fluctuations generated by thermal plumes, we showed in [27] that the $P^\star(Ra)$ dependence for $Ra > 10^{12}$ also appears in contradiction with the increase of degrees of freedom expected in the hard-turbulence regime. The observation suggest that the regime above $Ra \sim 10^{12}$ is no longer the hard-turbulence one.

Nature of the high-Ra regime. – *A priori*, a change in the dynamics of the large-scale circulation could possibly originate an increase of the plate's fluctuations, but a systematic investigation of the Reynolds number of the mean flow from $Ra = 10^7$ up to 10^{14} did not reveal such change in this cell [6]. In fact, the possible interpretations of the present results are strongly constrained by another observation: the increasse of the plate's fluctuations is concomitant with the increase of heat transfer. If we assume that this coincidence is not accidental, both events should be signatures of a common underlying change taking place in the cell. To the best of our knowledge,

only one interpretation presently accounts for the heat transfer increase, while staying consistent with all the other features reported in this cell. This interpretation —recalled in the introduction— states that the boundary layers undergoes a laminar-to-turbulent transition. It remains consistent with present results as one expects a boundary layer unstability to enhance the fluctuations of the temperature drop δT_{bl} across it. This is a central outcome of this paper.

Conclusion. – A constant heating is applied to the bottom plate of a Rayleigh-Bénard cell and this plate's temperature fluctuations are analysed. We focus on times scales larger than typically 2 turn-over times of the large scale circulation.

Below $Ra \simeq 10^{12}$, we give evidence that the plate's fluctuations follow the temperature fluctuations of the bulk of the cell. This implies that the temperature drop across the bottom boundary layer has negligible low-frequency fluctuations. Above $Ra \simeq 2 \times 10^{12}$, the bottom-plate fluctuation abruptly increase compared to the fluctuations in the bulk. This change is interpreted as an extra noise contribution raising across by the boundary layer. We discussed and discarded the possibility that this noise was present but simply masked at lower Ra. The negative skewness of the plate's temperature fluctuations —whose absolute value quickly increases in the high-Ra regime— seems incompatible with the trend toward gaussianity expected in hard-turbulence regime. This observation also indicates the occurence of a specific flow regime above $Ra \sim 10^{12}$.

A transition of the heat transfer law has already been reported for the same threshold Ra with this cell [1]. It has been interpreted as the triggering of Kraichnan's Ultimate Regime of convection, which is associated with a laminar-to-turbulent transition of the boundary layer [5]. This interpretation, which implies an instability of the boundary layer, also accounts for the present results, since such an instability is expected to enhance fluctuations in the boundary layer.

* * *

We thank B. Chabaud, B. Hébral, S. Aumaitre, P. Diribarne, Y. Gagne, and more especially B. Castaing for discussions and inputs. We thank the authors of [1] for sharing their raw data. This work was made possible thanks to the Région Rhône-Alpes support under contract 301491302.

REFERENCES

[1] Chavanne X., Chillà F., Castaing B., Hébral B., Chabaud B. and Chaussy J., *Phys. Rev. Lett.*, **79** (1997) 3648.

[2] Roche P.-E., Castaing B., Chabaud B. and Hébral B., *Phys. Rev. E*, **63** (2001) 045303(R) 1.

[3] Niemela J. J. and Sreenivasan K., *J. Fluid Mech.*, **481** (2003) 355.

[4] Roche P.-E., Gauthier F., Chabaud B. and Hébral B., *Phys. Fluids*, **17** (2005) 115107.

[5] Kraichnan R., *Phys. Fluids*, **5** (1962) 1374.

[6] Chavanne X., Chillà F., Chabaud B., Castaing B. and Hébral B., *Phys. Fluids*, **13** (2001) 1300.

[7] Schlichting H., *Boundary-Layer Theory*, 8th edition (Springer, New York) 2000.

[8] Wu X.-Z., *Along a road to developed turbulence: free thermal convection in low temperature helium gas,* PhD Thesis, University of Chicago (1991).

[9] Ashkenazi S. and Steinberg V., *Phys. Rev. Lett.*, **83** (1999) 3641.

[10] Niemela J. J., Skrbek L., Sreenivasan K. and Donnelly R., *Nature*, **404** (2000) 837.

[11] Procaccia I., Ching E. S. C., Constantin P., Kadanoff L. P., Libchaber A. and Wu X.-Z., *Phys. Rev. A*, **44** (1991) 8091.

[12] Niemela J. J. and Sreenivasan K. R., *J. Fluid Mech.*, **557** (2006) 411.

[13] Kenjereš S. and Hanjalić K., *Phys. Rev. E*, **66** (2002) 036307.

[14] Amati G., Koal K., Massaioli F., Sreenivasan K. and Verzicco R., *Phys. Fluids*, **17** (2005) 121701.

[15] Landau L. and Lifshitz E., *Fluid Mechanics*, 2nd edition, *Course of Theoretical Physics*, Vol. **6** (Pergamon Press) 1987.

[16] Niemela J. J., Skrbek L., Sreenivasan K. R. and Donnelly R. J., *J. Low Temp. Phys.*, **126** (2002) 297.

[17] Gauthier F., Hébral B., Muzellier J. and Roche P.-E., in *Advances in Turbulence XI, Proceedings of the 11th EUROMECH European Turbulence Conference, June 25–28, 2007, Porto, Portugal*, edited by Palma J. M. L. M. and Silva Lopes A., *Springer Proc. Phys. Ser.*, Vol. **117** (Springer, Heidelberg) 2007, p. 645.

[18] Roche P.-E., Castaing B., Chabaud B., Hébral B. and Sommeria J., *Eur. Phys. J. B*, **24** (2001) 405.

[19] Chavanne X., Chillà F., Chabaud B., Castaing B., Chaussy J. and Hébral B., *J. Low Temp. Phys.*, **104** (1996) 109.

[20] Mc Carty R. and Arp V., *Advances in Cryogenic Engineering*, edited by Fast R. W., Vol. **35** (Plenum Press, New York) 1990, p. 1465.

[21] Roche P.-E., Castaing B., Chabaud B. and Hébral B., *J. Low Temp. Phys.*, **134** (2004) 1011, cond-mat/0307518.

[22] Lu L., Yi W. and Zhang D. L., *Rev. Sci. Instrum.*, **72** (2001) 2996.

[23] Chillà F., Rastello M., Chaumat S. and Castaing B., *Phys. Fluids*, **16** (2004) 2452.

[24] Niemela J. J., Skrbek L., Sreenivasan K. R. and Donnelly R. J., *J. Fluid Mech.*, **449** (2001) 169.

[25] Wu X.-Z. and Libchaber A., *Phys. Rev. A*, **45** (1992) 842.

[26] Aumaître S. and Fauve S., *Europhys. Lett.*, **62** (2003) 822.

[27] Gauthier F. and Roche P.-E., arXiv: 0801.4830 (2008).